LIMNOLOGY and OCEANOGRAPHY: METHODS

ASLO

Limnol. Oceanogr.: Methods 21, 2023, 192–208

doi: 10.1002/lom3.10539

Combining quadrat, rake, and echosounding to estimate submerged aquatic vegetation biomass at the ecosystem scale

Morgan Botrel [1,2]* **Christiane Hudon** [2,3] **Pascale M. Biron** [2,4] **Roxane Maranger** [1,2]

[1]Département de Sciences Biologiques, Université de Montréal, Complexe des Sciences, Montreal, Quebec, Canada
[2]Groupe de Recherche Interuniversitaire en Limnologie (GRIL), Montreal, Quebec, Canada
[3]Environment and Climate Change Canada, Water Science and Technology, Montreal, Quebec, Canada
[4]Department of Geography, Planning and Environment, Concordia University, Montreal, Quebec, Canada

Abstract

Measuring freshwater submerged aquatic vegetation (SAV) biomass at large spatial scales is challenging, and no single technique can cost effectively accomplish this while maintaining accuracy. We propose to combine and intercalibrate accurate quadrat-scuba diver technique, fast rake sampling, and large-scale echosounding. We found that the overall relationship between quadrat and rake biomass is moderately strong (pseudo $R^2 = 0.61$) and varies with substrate type and SAV growth form. Rake biomass was also successfully estimated from biovolume (pseudo $R^2 = 0.57$), a biomass proxy derived from echosounding. In addition, the relationship was affected, in decreasing relevance, by SAV growth form, flow velocity, acoustic data quality, depth, and wind conditions. Sequential application of calibrations yielded predictions in agreement with quadrat observations, but echosounding predictions underestimated biomass in shallow areas (< 1 m) while outperforming point estimation in deep areas (> 3 m). Whole-system quadrat-equivalent biomass from echosounding differed by a factor of two from point survey estimates, suggesting echosounding is more accurate at larger scales owing to the increased sample size and better representation of spatial heterogeneity. To decide when an individual or a combination of techniques is profitable, we developed a step-by-step guideline. Given the risks of quadrat-scuba diver technique, we recommend developing a one-time quadrat–rake calibration, followed by the use of rake and echosounding when sampling at larger spatial and temporal scales. In this case, rake sampling becomes a valid ground truthing method for echosounding, also providing valuable species information and estimates in shallow waters where echosounding is inappropriate.

Submerged aquatic vegetation (SAV) provides many aquatic ecosystem functions and services, from stabilizing sediments to maintaining critical habitat for fauna (Carpenter and Lodge 1986; Hilt et al. 2017). Ecosystem service provisioning by SAV meadows is dependent both on plant patch density and size where high elemental fluxes and faunal populations are associated with high SAV standing stock (Cyr and Downing 1988; Rooney et al. 2003; Brown et al. 2004). However, SAV standing stock is sensitive to human pressures with, for example, declining SAV abundance in shallow lakes mainly reflecting loss of water transparency caused by increasing eutrophication (Scheffer et al. 1993). Management efforts around SAV thus often attempt to restore abundant meadows, while invasive alien aquatic "weeds" that impede multiple water usages are typically actively removed (Hussner et al. 2017; Madsen and Wersal 2017). Regardless of the management needs, accurate estimates of SAV standing stock are essential to assess their overall functional role in ecosystems and whether management strategies are working.

SAV standing stock or standing biomass is the density measure of aboveground living plant material in mass per unit area. Biomass can be either measured using destructive removal techniques or estimated using remote sensing (Fig. 1a). Destructive techniques consist of harvesting plant material, either from below or above the water surface. These are measures of direct

*Correspondence: morganbotrel@gmail.com

Author Contribution Statement: All authors contributed to the study design. C.H., R.M., and M.B. were responsible for field work and data acquisition with C.H. providing all quadrat data and much of rake data. M.B. was responsible for data curation, conducted data analysis, and wrote the original draft, while R.M, C.H., and P.B. reviewed and edited the manuscript.

Additional Supporting Information may be found in the online version of this article.

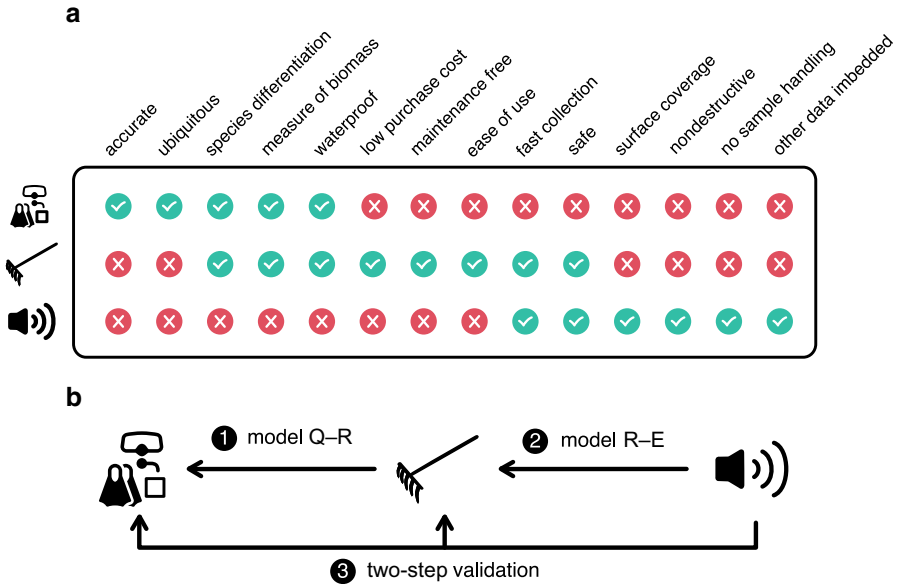

Fig. 1. Comparison and combination of the quadrat, rake, and echosounding techniques to estimate SAV biomass. (**a**) Strengths and weaknesses of the different techniques. (**b**) Approach and steps to combine techniques. Q, quadrat; R, rake.

biomass, as opposed to a proxy, and represent SAV biomass spatially as a point phenomenon. Direct underwater harvest of SAV by scuba divers is the biomass measure with the least bias (Downing and Anderson 1985; Madsen 1993). It is thus the most accurate biomass measure and also has the advantage of being applicable at all depths. However, this technique requires specialized scuba training. In addition, because of long collection time, small quadrat size (< 1 m^2), and the associated safety risks and expenses, sampling of large areas or in turbid waters is not possible. To alleviate these shortcomings, destructive techniques using tools to grab samples from the surface have been developed. Multiple tools exist, but the double-headed rake with a variety of assembly features (on a telescopic pole, tongs or rope) and collection methods (dragged, griped or spun) is rather well adapted for use in large surveys (Rodusky et al. 2005; Johnson and Newman 2011; Yin and Kreiling 2011; Madsen and Wersal 2017). Indeed, the rake is convenient for large-scale recurrent SAV sampling due to its low purchase cost, ease of use, fast collection, robustness, and simple maintenance. However, rake collection is restricted to shallow depths (< 3–4 m) and is biased since plant material is often not entirely collected or collected in excess (Rodusky et al. 2005; Kenow et al. 2007; Johnson and Newman 2011). Furthermore, all destructive methods are point measurements and require the collection and processing of multiple replicates to reach a reasonably precise estimation at a given site due to the typical patchy distribution of SAV meadows at small scale (Downing and Anderson 1985). Accurate measurements of SAV biomass capturing SAV heterogeneity at larger spatial scales thus remain a challenge, since surveys using quadrats are accurate but only applicable at small scale whereas rake samples are more biased but provide a broader estimate of biomass distribution.

At large spatial scales, SAV biomass estimates can be improved with remote sensing that represent SAV in space as a continuous surface phenomenon. These techniques provide a proxy of biomass where SAV is detected by a receiver that captures a signal (e.g., sound or light) reflected or emitted by SAV (Rowan and Kalacska 2021). Capturing the sound reflection made by gas vacuoles in plant tissue (the echo) using an active single beam echosounder, is the simplest and best remote sensing technique to estimate SAV biomass in turbid freshwaters (Duarte 1987; Sabol et al. 2002; Vis et al. 2003; Rowan and Kalacska 2021). Indeed, echosounders are transportable and increasingly affordable devices that, just like a sonar used for fishing, can be hooked on the side of a boat for a rapid, nondestructive and repeatable survey (Howell and Richardson 2019). The reflection of sound on bottom surfaces and canopies allows for the simultaneous measurement of SAV height and water depth, which is extremely useful as water depth strongly influences SAV biomass (Duarte and Kalff 1990). Because SAV height correlates to biomass, echosounding has successfully been used to model whole community biomass (Maceina et al. 1984; Duarte 1987; Sabol et al. 2002). However, the allometric relationship between height and biomass varies with species growth form and thus the calibration of SAV echo is species- or stand-specific and as such the measurement needs to be repeated frequently (Duarte 1987). Other drawbacks of echosounding include its lack of species differentiation, inability to take measurements in very shallow waters (< 0.4–0.7 m) or when plants reach water surface, and obligate sampling during calm weather conditions, since wind-induced gas bubbles strongly scatter

sound (Sabol et al. 2002). Furthermore, the use of echosounding requires technical expertise, from maneuvering the instrument, electronic maintenance to processing data output.

Each of the aforementioned techniques has several advantages and disadvantages for estimating SAV biomass depending on the scale of study (Fig. 1a). One promising approach would be to design a process enabling the benefits of all three techniques which could provide accurate biomass estimates that take SAV heterogeneity at broad spatial scales into account. Therefore, our objective is to develop a process that assesses the interchangeability of quadrat, rake, and echosounding techniques to render their use synergistic and both time and cost-effective. To do so, we conducted two intercalibrations: one between biomass from quadrat and rake and the other between rake and a biomass proxy derived from echosounding (Fig. 1b). Furthermore, we investigated how the predictions of both intercalibrations models are affected by environmental factors. The resulting two models were then sequentially applied to echosounding data to validate our approach. Finally, we assessed how increasing the sample size using echosounding modifies whole-system biomass estimation and provide a decision-making tool adapting the methods to study purpose.

Materials and procedures

To compare, and integrate the different biomass assessment techniques, three datasets were used: the quadrat–rake (Q–R), the rake–echosounding (R–E), and the validation datasets (Table 1). All datasets were collected in Lake Saint-Pierre (LSP), a $\sim$ 300 km^2 widening of the Saint-Lawrence River in Quebec, Canada (Fig. 2a, b). Part of the Q–R dataset was also collected in the nearby upstream fluvial lakes, Saint-Louis and Saint-François.

Q–R dataset

The first dataset was used to assess the correspondence between biomass estimates derived from quadrat and rake samples. We had to compare destructive techniques that were measured on distinctively sampled area but representative of the same site. Given that at the time of the sampling such a comparison had yet to be done, we tested three different collection strategies: systematic pairs, haphazard pairs or blocks (Fig. 2c). For the first two strategies, paired rake and quadrat samples were collected around the anchored boat, using either a systematic or a haphazard strategy. In the "systematic pair" strategy, a single quadrat (0.25 m $\times$ 0.25 m) was systematically collected to the upper right side of each rake sample (1 m $\times$ 0.35 m). In the "haphazard pair" strategy, bigger quadrats (0.40 m $\times$ 0.60 m) were located in the vicinity of the rake sample site. In the block sampling strategy, a block, which consisted of two rake samples positioned on both sides of a row of four individual quadrats (0.25 m $\times$ 0.35 m each) aligned to mimic the raked area, was collected on each side of the boat.

Quadrat plant samples were harvested by divers from within a polyvinyl chloride (PVC) frame placed on the lake bottom by divers. All aboveground plant material was cut using grass-clippers or broken at the sediment surface. Rake samples were collected from the anchored boat, using a double-headed rake (0.35-m head width with 14, 8-cm long teeth on both sides) mounted on a telescopic pole (maximum length 5 m) following the method described by Yin and Kreiling (2011). The rake was lowered in the water and dragged toward the boat over the bottom on a length of approximately 1 m. As it was lifted from the water, the rake was flipped 180° to minimize plant loss.

Biomass samples were collected during the period of maximum SAV development during the summers of 2006–2009. Sites were chosen to cover a wide range of water depths, sediment types, and SAV biomass. Water depth at each site was measured with a survey ruler and sediment type was classified as pebble, sand, silt, clay, or a mixture thereof. SAV species composition of each sample was visually assessed in decreasing abundance rank (1 = most abundant species). Plant material was washed on site to remove sediment and debris prior to further processing (on site, in the laboratory on fresh or thawed samples). Macrophytes (vascular plants and macroalgae such as *Nitella* and *Chara* spp.) were separated from filamentous algal mats (Chlorophytes or the cyanobacterium *Microseira* (*Lyngbya*) *wollei*); each group was wrung out manually and either weighted with a hook-scale on site (precision 0.02 kg) or an electronic scale in the laboratory (precision 0.1 g). A subsample of filamentous algae was preserved in lugol for subsequent microscopic identification ($\times$250). Wet mass was converted to dry mass using previously established conversion factors for SAV (Hudon et al. 2012) and filamentous species (Cattaneo et al. 2013). All of the manipulations from sample collection to final biomass conversion are referred to "biomass treatments."

Both biomass and species information were aggregated per site. Biomass measurements were reported as a mean of 3–5 rake and quadrat replicates for the systematic and haphazard pair collection strategies or on two rakes and four quadrats for the block collection strategy. Species information per replicate sample was converted to dominant growth form type as either species forming dense canopy, short understory species or species with leaves growing from a basal rosette, using the dominant species only (rank 1). Canopy-forming plants (< 3 m) included mainly *Potamogeton richardsonii* but also *Heteranthera dubia*, *Stuckenia pectinata*, *Elodea* spp., and *Myriophyllum* spp. *Chara* spp. formed a low-lying (< 20 cm) layer on the bottom, while *Vallisneria americana* formed rosette of linear leaves extending toward the surface (< 1.5 m). When more than half of the replicates at a given site had the same dominant growth form, that growth form was allocated to the site.

R–E dataset

The second dataset was used to predict rake biomass from echosounding. Both acoustic and rake surveys were carried out in the southwest portion of LSP once a year from 2012 to

Table 1. Summary of the three datasets used in this study.

	Q–R	Rake–echo	Validation
Location	LSP 46°09′N 72°52′W LSL 45°24′N 73°54′W LSF 45°08′N 74°21′W	LSP 46°09′N 72°52′W	LSP 46°09′N 72°52′W LSP 46°13′N 72°53′W
Year	2006–2009	2012–2017	2013, 2016
Time of biomass collection	Jul, Aug, Sep	26–28 Jun (2012 only) 27 Jul to 17 Aug	13–16 Aug 2013 16–25 Aug 2016
Time of echosounding		18–20 Jun (2012 only) 27 Jul to 15 Aug	12–13 Aug 2013 3–4 Aug 2016 and 01–02 Sep 2016
Biomass treatment	Fresh and frozen/thawed	Frozen/thawed	Frozen/thawed and fresh
Species identification	Visual abundance rank	Biomass per species	Biomass per species
Type of comparison	3 dispositions systematic pair, haphazard pair, block	Constant distance to rake station	Constant distance to quadrat station
Number of biomass site	77	217	105
Size of the quadrat sampling unit (m)	0.25 × 0.25 0.40 × 0.60 0.25 × 0.35		0.25 × 0.25 0.30 × 0.30 (at low SAV density 1–100 m^2)
Size of the rake sampling unit (m)	0.35 × 1	0.35 × 1	
Biomass replicates per site	3–5 or 2–4	3–5	3
Variables used in analysis	Quadrat biomass Rake biomass Collection strategy Biomass treatment Lake Substrate type Depth Growth form	Rake biomass Biovolume Biovolume SD Depth Growth form Chlorophyte biomass *Microseira* (*Lyngbya*) *wollei* biomass Number of ping report Mean distance to rake site Flow velocity Wind speed Wind direction	Quadrat biomass Biovolume Biovolume SD Depth

LSF, Lake Saint-François; LSL, Lake Saint-Louis.

2017 during the moment of maximum biomass, but also once early in the growing season in June 2012 (Fig. 2b,d). Acoustic surveys were conducted on 250-m-spaced transects perpendicular to the lake shore at low and constant speed (~ 1.1 m s^{-1}). Acoustic data were collected using a downward-looking BioSonics single beam transducer mounted on an Ocean Science riverboat fixed to the side of the vessel by a steel rod. This setup allowed the transducer to be constantly immersed below 5 cm of the water surface. Floating and drifting vegetation frequently became entangled with the transducer, which consequently was regularly cleaned. The transducer had a beam angle of 6.6° and a working frequency of 430 kH, which depending on water depth, represents a circle of 0.10 to 0.20 m cone diameter of sound reaching the sediment surface. Echosounding was controlled by a BioSonics DTX system running Visual Acquisition 6.06 with a pulse length of 0.1 ms and a ping rate of 5 ping s^{-1}. Geolocation data were simultaneously recorded with a GNSS NovAtel Smart V1 receiver placed on top of the transducer. Real-time differential correction was obtained using the Omnistar VBS network in 2012 and 2013 (0.90 m precision) and the WAAS network in 2014–2017 (0.65 m precision). Acoustic data (echograms and geographic coordinates) were saved in dt4 files on a laptop PC for postprocessing.

Acoustic data were processed using Visual Habitat 1. Lake bottom was first determined using a rising edge threshold of −47 dB and a rising edge length criterion of 10 cm. The resulting delineations on the echograms were manually corrected to have a bottom line following highest amplitudes. SAV was subsequently analyzed using plant detection threshold above ambient noise of −68 dB and a minimum height of plant detection of 10 cm. SAV delineations were again

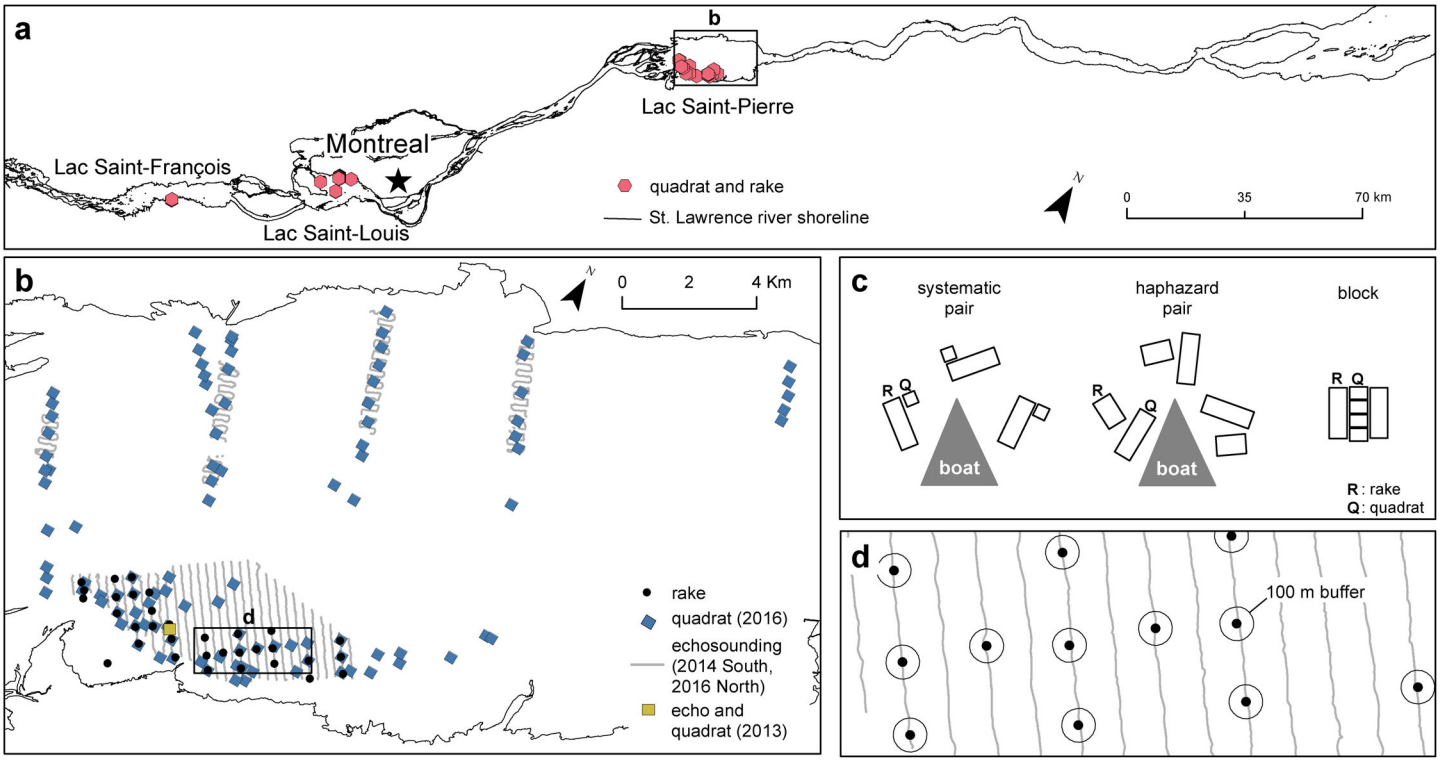

Fig. 2. (**a**) Sampling locations in the St. Lawrence River for the Q–R dataset; (**b**) R–E and validation (echosounding–quadrat) datasets in Lac Saint-Pierre. (**c**) collection strategy to compare quadrat to rake; (**d**) collection strategy to compare rake to echosounding. For the R–E dataset in (**b**), 2014 rake sampling sites and echosounding tracks are shown as an example (South-West sector). To clearly visualize the validation dataset in (**b**), all the 2016 quadrats (blue diamonds) are depicted but only part of the 2016 echosounding tracks (North section, South-West tracks are similar to R–E dataset) and the general location of the 2013 small scale sampling (yellow square, South-West sector) are shown.

manually corrected when the plant line was going beneath the bottom line, mainly due to false detection of plants reaching the water surface. Invalid ping reports were removed, and remaining reports were exported for cycles of five pings to have a sample resolution similar to the raked length and a data point every ~ 1.1 m. For each cycle, mean plant height (m), plant cover (%), mean geographic position (decimal degree), and mean depth (m) were exported. SAV biovolume, a potential proxy of SAV biomass, was computed as mean plant height × mean plant cover.

Within 1–2 weeks of the acoustic surveys, rake samples were collected at 35 sites along the echosounding transects. Sites were positioned using a Trimble GeoXT (precision 0.50 m) in 2012–2013, a SXBlue II GPS (precision 0.65 m) in 2014–2015, and a Garmin 64 S (precision 3 m) in 2016 and 2017. Water depth (z) was measured with a survey ruler and, to be comparable with depth during echosounding, was corrected using the equation $z = z_{\text{rake}} - \text{lvl}_{\text{date rake}} + \text{lvl}_{\text{date echo}}$ and water level (lvl) at station 15975 (Fisheries and Ocean Canada, www.isdm-gdsi.ca, accessed 27 November 2017). Depth average flow velocity was also measured at the time of or one week prior to biomass sampling. Velocity was measured at 60% of site depth using a rotating (Swoffer 3000) or electromagnetic (Marsh McBirney Flo-mate 2000 or Valeport model 801) flowmeter. At each site, 3–5 rake replicates were collected around the anchored, 7-m long boat, using the same apparatus and dragged length as the Q–R dataset. To ensure that a location was not raked twice, rakes were systematically collected in front and on each side of the boat and as distant as possible when replicate number exceeded three. Plant material was similarly processed as described for the Q–R dataset, but plants were sorted by species in the lab and macrophyte biomass was measured on dried material. Total SAV biomass was computed from the species biomass and pooled by growth form. The same species as the Q–R dataset were found. All SAV biomass herein are reported as mean dry biomass in g m^{-2}.

Since rake collection and echosounding of the same SAV sites were conducted independently, we determined the spatial resolution at which they could be compared by inspecting the relationship between rake biomass and mean biovolume at increasing radial distance from the rake site (*see* Supporting Information Text S1; Fig. S1). We performed this comparison at radial distances ranging from 1 to 100 m (Fig. 2d), and a resolution of 20 m (or 10-m radius around rake site) was selected based on an observed higher correlation with field observations. Using the 20 m resolution, we calculated the biovolume

standard deviation (SD) as an indicator of the acoustic error, the mean ping report distance to rake site as the acoustic proximity, and the number of ping reports per site as the acoustic frequency.

Validation dataset

The third dataset was used to validate biomass estimation from echosounding and compare it to quadrat biomass. Acoustic and quadrat surveys were carried at the time of maximum biomass accumulation in 2013 and in 2016. In 2013, the survey was concentrated in a small (100 m × 100 m) area of high biomass in southwest LSP characterized by a narrow depth range (1.4–1.5 m; Fig. 2b). In 2016, the survey was conducted in both the southwest and the northern sector of LSP. The northern sector was characterized by greater depth range (0.5–7.0 m). Quadrat sampling in this sector was carried in five transects and the 250 m-spaced echosounding transects were perpendicular to the quadrat transects. The southwest sector had shallower depths (< 2.7 m), and echosounding transects were selected following the same methodology as described for the R–E datasets. Processing of acoustic data and biomass samples were also conducted similarly to the R–E dataset, but aboveground biomass was collected in triplicates by scuba divers using a 0.30 m × 0.30 m quadrat in 2013, a 0.25 m × 0.25 m quadrat in 2016, and balance precision was 0.0004 kg. When SAV density was very low, divers evaluated the surface they patrolled without plants as a straight line or a circle around the anchor (up to 100 m^2) and collected the few plants they found. Quadrat and echosounding were spatially matched using the same resolution of 20 m determined from the R–E dataset.

Statistical analysis

To predict quadrat biomass from rake biomass, we conducted two distinct analyses with different purposes. First, to derive mean parameter estimates while allowing for a hierarchical structure, we used linear mixed modeling (LMM) with Gaussian error. Only rake biomass was included as the fixed effect, and the random terms were date and sampling site. The random effect models were fitted with restricted maximum likelihood estimation and selected to minimize the sample-corrected Akaike information criterion (AICc) following the approach of Zuur et al. (2009). To assure the selected model captured spatial autocorrelation, absence of correlation was assessed by looking at correlograms of model residuals. Second, we investigated how environmental variables affected the rake and quadrat biomass relationship. The intention was to indicate which variable should be controlled for or included in the intercalibration to reach a higher accuracy. Given that available variables were mostly categorical (collection strategy, biomass treatment, lake, substrate type, and growth form, Table 1), we tested this using analysis of covariance (ANCOVA). When the relationship between quadrat and rake biomass exhibited different slopes and intercepts for a given condition, separate regression equations were computed for each category using ordinary least square regression. We also evaluated the effect of depth on the quadrat–rake biomass relationship using partial regression.

We applied a similar two-analysis approach to predict rake biomass from echosounding biovolume. LMM was used to derive mean parameter estimates, but to describe how environmental variables affected the rake biomass and biovolume relationship, we used partial least square regression (PLSR). This method was chosen based on the structure of the dataset that included many continuous and potentially correlated variables. Variables included in the analysis described SAV growth form, macroalgae abundance, water depth, flow velocity, wind (hourly wind speed and direction acquired from Meteorological Service of Canada, climate.weather.gc.ca, accessed 27 November 2017) and acoustic data quality during surveys (Table 1). This method allowed us to visualize in reduced space the multiple covariates and is also robust when there is high collinearity among many predictors and when numbers of observations are low (Mevik and Wehrens 2007). For this, we selected components using the leave-one-out cross-validation and the one-sigma heuristic approach. We then selected variables using the filter method of selectivity ratio (SR), which is the ratio of the explained to the residual variance of the *X* variables on the y target projection. We chose SR over the commonly used variable importance of the projection (VIP) because the former selects important variables using a *F*-test and performs well for prediction (Farrés et al. 2015).

To validate our intercalibration approach, we applied our models in two steps. First, from echosounding biovolume, we predicted rake biomass and from that estimation we predicted quadrat biomass. We propagated model error with Monte Carlo simulations and used the root mean square error (RMSE) of the LMM residuals as the model error term. Second, we visually compared in space the quadrat-equivalent biomass predicted from echosounding to measured quadrat biomass. For this, we created spatially interpolated biomass maps from both quadrat and echosounding using kriging.

To compare the effect of sample size and spatial coverage on whole-system biomass, we compared biomass estimate from point sampling to remote sensing using the R–E dataset over five summer campaigns. We first calculated mean biovolume along echosounding transects in 20 m distance bins. We then created a spatial polygon for each campaign where both rake and echosounding had a good spatial coverage. To do so, we intersected two 100 m buffers around concave hulls created from the rake sites and echosounding sites. Within the intersected spatial polygon, mean biomass for rake and echosounding sites were then calculated with bootstrapping confidence intervals. This resampling technique has been shown to be more appropriate for estimating seaweed confidence intervals and is particularly suitable when the true distribution of the data is unknown or skewed (Johnson 2020). For echosounding, we also estimated a spatially interpolated average.

Due to high SAV heterogeneity ranging from bare patches to dense plant abundance, absence data (where quadrat or rake biomass = 0 and biovolume = 0) were excluded from modeling analysis. The three techniques had different sample unit size and sampling effort (Table 1). Therefore, techniques with higher sample unit size, for example, rake, or having a higher number of observations, for example, echosounding, had a higher probability of finding SAV in low biomass regions compared to their correspondent explained variable (e.g., quadrat and rake, respectively). The resulting models to predict rake and quadrat biomass were applied only to presence data (biovolume > 0 or rake biomass > 0) and absence recorded by both techniques were deemed true. When necessary, data used in statistical analyses were transformed to respect assumptions of normality. Data handling and statistical analyses were performed in R 3.6.3 (R Core Team 2020). LMMs were computed with the lme4 package (Bates et al. 2015), with AICc compared using the MuMIn package (Bartoń 2020). PLSR with variable selection was carried out using pls and plsVarSel (Mehmood et al. 2012; Mevik et al. 2020). Geospatial data were handled using the sp, sf, raster, and concaveman packages (Pebesma and Bivand 2005; Pebesma 2018; Gombin et al. 2020; Hijmans 2020), while geostatistical modeling and kriging were performed using gstat (Pebesma 2004). Bootstrapping confidence intervals were computed using the boot package (Canty and Ripley 2021).

Assessment

Prediction of quadrat biomass using rake samples

The overall relationship between quadrat biomass and rake biomass was moderately strong with a pseudo R^2 of 0.61 (Fig. 3a; Table 2; Supporting Information Table S1). The selected random effect of sampling site accounted for an additional 9% of variation (Supporting Information, Tables S2, S3). The quadrat and rake distributions were skewed, leading to non-normal regression residuals, therefore the modeled relationship was on $\log_{10}$ data. The quadrat biomass was generally significantly higher by a factor of 4 than biomass estimated using a rake ($\text{median}_Q = 55\ g\ m^{-2}$, $\text{median}_R = 14\ g\ m^{-2}$, paired t-test $p < 0.0001$). Quadrat estimates had 20 times higher variance (median $s^2_R = 537\ g\ m^{-2}$, median $s^2_Q = 30\ g\ m^{-2}$, $p < 0.001$) than rake equivalents, resulting in a higher standard error (SE, median $SE_Q = 10\ g\ m^{-2}$, median $SE_R = 4\ g\ m^{-2}$). There was a correlation between mean biomass and its associated error for both quadrat and rake ($r_Q = 0.82$, $r_R = 0.77$), indicating that the difference in error between methods could be caused by the higher biomass measured in quadrat sampling. Furthermore, this inflation of error with biomass was not constant: the ratio of variance to mean biomass ($s^2/\bar{x}$) increased with mean biomass and was generally higher for quadrat than rake ($\bar{x}_Q = 41$, $\bar{x}_R = 17$). As a result, both rake and quadrat measurements showed a spatial aggregation of biomass ($s^2 > \bar{x}$), although more markedly so for quadrats (99% of observations) than for rakes (67% of observations).

The discrepancy between rake and quadrat biomass comparison was not constant over the biomass gradient (Fig. 3a; Table 2). The slope was less than one (0.64) and rake underestimation of quadrat biomass was highest at low biomass, while measurements from both methods converged at higher biomass ($> \sim 100\ g\ m^{-2}$). The intercept was greater than 0 ($\log_{10}$[quadrat biomass] = 0.96 or quadrat biomass = $8\ g\ m^{-2}$), therefore application of the equation would result in systematically biased biomass estimation in the absence of SAV and has to be limited to presence data (Table 2).

Predictions of quadrat biomass from rake measurements were affected by substrate type and SAV growth form (Fig. 3b,c), while no effect of collection strategy, biomass treatment, lake or depth was detected. The slopes and intercepts of the relationship differed significantly among substrate type ($F_{2,61} = 4.44$, $p = 0.02$), with silt displaying a higher intercept, lower slope and higher variability than sandy sediments (Table 1). This was indicative of the greater efficiency of rake to collect SAV, especially at low biomass, in sand bed areas compared to finer and more organic sediments (silt). For sandy sediments, the slope was not only closer to one, but the relationship also had a better fit. In hard packed sediments (clay–pebble), rake sampling seemed to be unsuited and completely failed to collect any plant material despite their known presence. However, this substrate type occurred only at a small number of sites ($n = 6$) and the biomass at these sites was very low ($< 0.5\ g\ m^{-2}$).

In the case of the effect of the dominant growth form, the relationship slopes were similar for rosette and canopy-forming SAV ($F_{1,42} = 0.02$, $p = 0.88$), but their intercepts were significantly different ($F_{1,43} = 6.93$, $p = 0.01$). Understory were dominant at only two sites and were excluded from analysis. For the same rake biomass, the rosette had a quadrat biomass systematically higher than canopy by $1.95\ g\ m^{-2}$. Thus, rake was more efficient at sampling canopy-forming plants and tended to underestimate the biomass of rosette-forming *V. americana*. Inclusion of the dominant SAV growth form in the model resulted in an overall better fit and lower prediction error.

Prediction of rake biomass from acoustic data

When comparing rake biomass to biovolume, the distinct scale of the two methods was more apparent than for the quadrat–rake comparison. SAV were more spatially aggregated when looking at biovolume with 98% of observations having a variance higher than its mean ($s^2 > \bar{x}$) compared to 50% for rake. Nevertheless, the relationship between rake biomass and biovolume was moderately strong with a pseudo R^2 of 0.57 (Fig. 4; Supporting Information Table S4). The following equation described the generalized relationship:

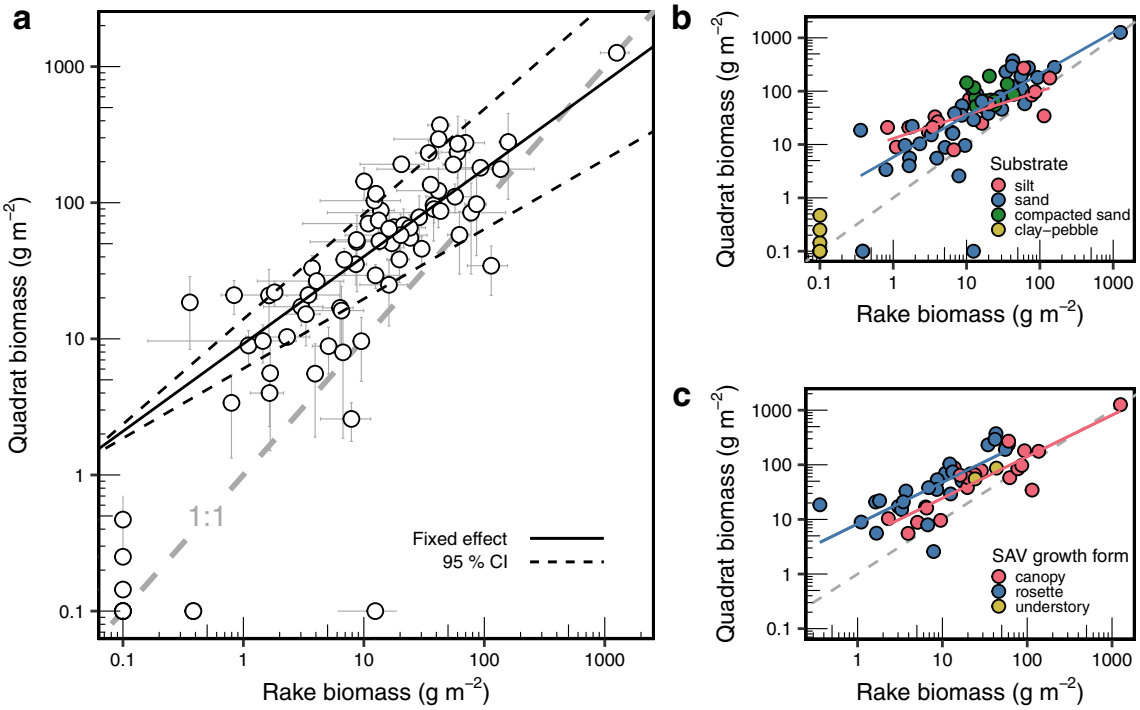

Fig. 3. Relationships to predict quadrat biomass from rake biomass. Overall relationship is shown in (**a**) and effect of substrate and growth form are shown in (**b**) and (**c**), respectively. Regression line is represented by the dark solid line with 95% confidence intervals as dashed lines and error bars are standard errors. Quadrat and rake absence (value displayed at 0.1) are depicted in (**a**) and (**b**) but are not included in regressions calculation.

$$\log_{10}\text{SAV rake biomass} = 0.37 \times \sqrt{\text{biovolume}} - 1.37 \quad (6)$$

An additional 27% of variation was explained by the selected random effect of varying intercept per sampling campaign and site (Supporting Information Tables S5, S6). This suggests that environmental conditions affected the rake biomass biovolume relationship. To test for this influence, we performed a PLSR (Fig. 4b,c). We first selected the number of components (or latent variables) for the PLSR using the RMSE of cross-validation (RMSECV), which had a minimal value of 0.60 ($\log_{10}$) at eight components. To avoid overfitting, we chose the model with three components (RMSECV = 0.63), which was the model with the fewest components that was less than one standard deviation from the best model (one-sigma heuristic approach). As expected, biovolume was the most important variables explaining these components (Fig. 4c). Biovolume SD was also a strong predictor, and like biovolume, it was correlated to rake biomass ($r_{\text{biovolume}} = 0.79$, $r_{\text{biovolume SD}} = 0.61$; Supporting Information Fig. S2a,b). The two echosounding variables were also correlated to one another ($r = 0.59$; Supporting Information Figs. S2c, S3a), although above a biovolume of 15, there was increased scatter

Table 2. Coefficients and summary statistics of models allowing to predict quadrat biomass ($\log_{10}$ g m^{-2}) from rake biomass ($\log_{10}$ g m^{-2}). Models are shown for all available data and for different subsets with distinct environmental conditions having a significant effect on the quadrat and rake relationship. 1|site indicates varying intercept per sampling site. For LMM, R^2 indicates the marginal R^2 (for the fixed effect).

Equation number	Environmental condition	Coefficients		R^2	n	Rake biomass range (g m^{-2})	Model type	Random effect
		Intercept	Slope					
1	All data	0.96	0.64	0.61	67	0.36–1257.68	LMM	1|site
2	Silt	1.11	0.44	0.46	16	0.84–136.45	OLS	
3	Sand	0.76	0.78	0.69	40	0.36–1257.68	OLS	
4	Rosette	0.92	0.76	0.61	26	0.36–59.91	OLS	
5	Canopy	0.63			20	2.30–1257.68	OLS	

OLS, ordinary least square.

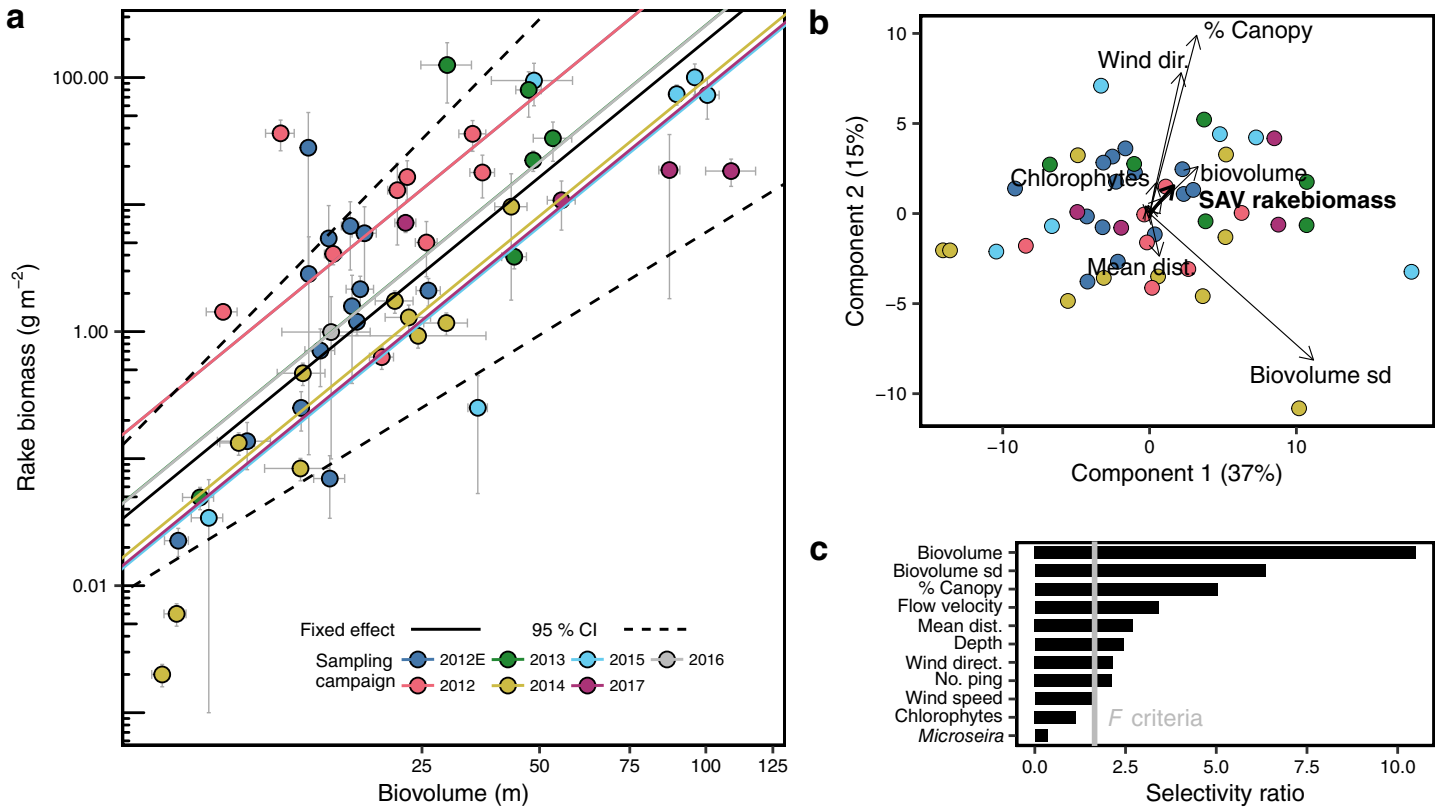

Fig. 4. Relationship to predict rake biomass from echosounding biovolume, and effect of environmental variability on the relationship. Overall fixed relationship is shown as a black line in (**a**) with the colored line showing the random effect of different intercept per sampling campaign. Gray lines radiating from points are standard errors. The effect of the environmental variables is shown in (**b**) as score plot of the PLSR model describing data configuration in relation to predictors, with the explained variable in bold. (**c**) The importance of environmental variables as predictors of rake biomass, with each variable's bar crossing the green line having a significant discriminant power at $p < 0.05$. CI confidence interval; dir. direction; dist. distance; no. number.

between the two variables and a reduced correlation ($r_{\text{biovolume}>4} = 0.10$). As a result, biovolume and biovolume SD were nearly orthogonal when looking at site configuration in relation to predictors (Fig. 4b). Biovolume was more highly correlated to rake SAV biomass and canopy growth form, while biovolume SD was pulled by two extreme data points. This suggest that biovolume SD does not add much predictive power compared to solely modeling rake biomass from biovolume.

Other potential predictors of rake biomass included, in decreasing order, SAV growth form, flow velocity, mean distance to rake site, depth and wind direction (Fig. 4c; Supporting Information Fig. S3b–f). Mean distance did not display any coherent patterns on the relationships between biovolume and rake biomass in contrast to other variables. The presence of canopy growth form modified the relationship, where canopy-forming plants had a higher rake biomass per biovolume than rosette-forming ones. Flow velocity was well correlated with biomass, where sites with lower flow had higher biomass. Depth seemed to induce a bias where shallow sites (< 1 m) tended to display a low biovolume for a given rake biomass. With regard to wind direction, sites sampled when winds were coming from North to North-West had high biovolume for their measured rake biomass.

Two-step model validation

To validate the two-step intercalibration approach, we predicted quadrat biomass by sequentially applying the general rake-biovolume Eq. 6 to echosounding data followed by the general the rake-quadrat Eq. 1 (Table 2). Predicted biomass was then compared to measured quadrat biomass. Three surveys carried out over different depth ranges were available for the comparison: a small-scale survey at constant depth (2013, 1.4–1.5 m), a survey in the deeper water in the North of LSP (0.5–7.0 m), and a survey in the shallow waters in the South of LSP (< 2.7 m). We first compared paired acoustic predictions at 10 m distance of quadrat measurements (Fig. 5). The two step predictions were comparable to the quadrat measurement and did not introduce any evident bias. The standard deviation of the Monte Carlo simulation was 4 g m^{-2} ($\log_{10}$ 0.59) which was an intermediate value between the RMSE of the two models (Q–R 1.9 g m^{-2} and R–E 2.4 g m^{-2}). However, the RMSE of the predictions 123 g m^{-2} was higher than the quadrat measured standard error (38 g m^{-2}). The

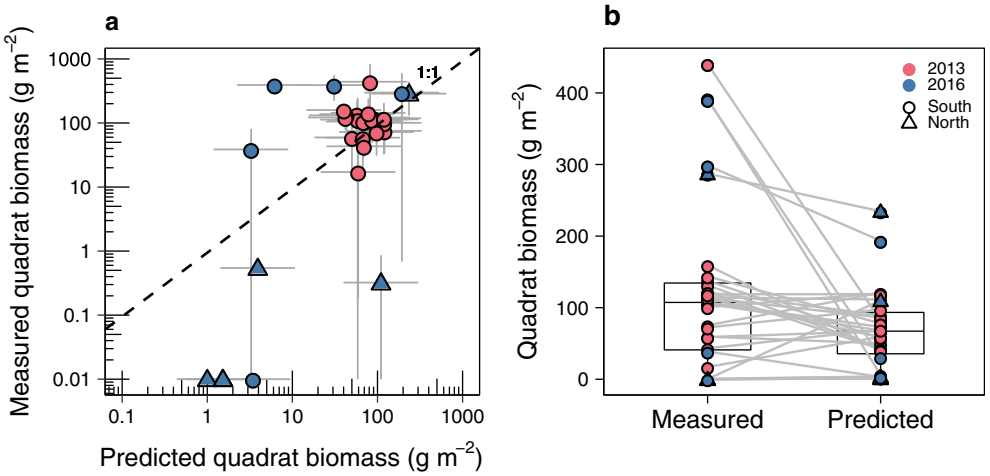

Fig. 5. Validation of the two-step quadrat biomass prediction from echosounding (using Eq. 1, Table 2 and Eq. 6 in text). (**a**) Scatterplot of measured vs predicted quadrat biomasses, error bars are the 95% confidence intervals and absence of measured biomass are depicted at 0.01 g m^{-2}. (**b**) Paired boxplot of measured vs predicted quadrat biomasses, solid horizontal line within boxes represents the median, boxes extent the 25th and 75th percentiles and whiskers the 10th and 90th percentiles.

mean absolute percentage error (MAPE) of the predictions was also higher than the relative error of the quadrat measurements (1333% vs. 50%, respectively), but it was driven by a single outlying data point in the North of LSP that, once removed yielded a MAPE of 87%. Indeed, when looking at each individual survey, the acoustic predictions in 2016 tended to have a higher error than the 2013 ones ($RMSE_{2016}$ = 166 g m^{-2}, $MAPE_{2016}$ = 5000%, $RMSE_{2013}$ = 95 g m^{-2}, $MAPE_{2013}$ = 51%). The 2016 predictions were either well above or below the 1 : 1 line, while the 2013 predictions from sites at a constant depth had a majority of their confidence intervals overlapping the 1 : 1 line. In 2016, sites from the deeper North sector tended to have higher predictions compared to nearly absent quadrat biomass (< 1 g m^{-2}). Echosounding integrates a larger number of measured units and thus better describes the same areal extent than quadrat (up to 400 m^2 vs. < 1 m^2) which, in this case, probably underestimates true biomass. Conversely, sites from the shallow South sector tended to have much lower acoustic predictions than that measured by quadrat, probably due to a bias from echosounding because of biomass accumulation at the surface from floating leaves. Overall, the predictions were not significantly different from quadrat measurements (paired *t*-test p = 0.17; Fig. 5b), although acoustic predictions had somewhat lower mean and median ($\bar{x}_{pred}$ = 68 g m^{-2}, $\bar{x}_{obs}$ = 121 g m^{-2}, $median_{pred}$ = 67 g m^{-2}, $median_{obs}$ = 107 g m^{-2}).

Second, given that most quadrat measurements in our dataset were located beyond 10 m from the echosounding track, we compared spatially interpolated measured quadrat biomass to interpolated predictions derived from echosounding (Fig. 6). In the 2013 constant depth range survey, the quadrat and echosounding estimation were very similar and small local differences were potentially caused by the higher sampling effort and surveyed area of echosounding (Fig. 6a,b). In the deeper North sector of LSP, interpolated biomasses were similar for quadrat and echosounding above the SAV maximum colonization depth (3 m, Fig. 6c,d). Echosounding clearly enabled the delimitation of SAV spatially because of a better accountability of limits imposed by depths. Quadrat interpolation tended to overestimate biomass in deeper waters where no sampling occurred. Conversely, in the shallow South (< 1.5 m, Fig. 6e,f), echosounding underestimated biomass, again probably because of bent SAV that accumulated at the water surface and prevented efficient estimation of underwater biomass using acoustic signal.

Effect of sample size on whole system estimation

Finally, we assessed how the increased sample size afforded by echosounding and the use of spatial interpolation method modify whole-system biomass estimation. Using the two models we developed, we predicted quadrat biomass from both rake biomass and biovolume for five independent SAV surveys where both rake sampling and echosounding had similar spatial extent. We then compared the mean from these estimated biomasses, either on the raw data or on spatially interpolated biomass (Fig. 7). In all surveyed years, the study area displayed heterogenous biomasses, with clear high and low biomass zones (Supporting Information Fig. S4). This combined with the different sampling effort of rake (n = 21–30) and echosounding (n = 1224–1934) created widely different mean biomass per survey. Biomass predicted from rake was, depending on the survey, either lower or higher than that from echosounding, generally by a factor of 2. The mean estimate of each technique was distinct and there was almost no overlap with their confidence intervals. As a result, the range across years of mean biomass from rake (15–59 g m^{-2}) was more limited compared to that from echosounding (9–84 g m^{-2}). The higher number of observations using

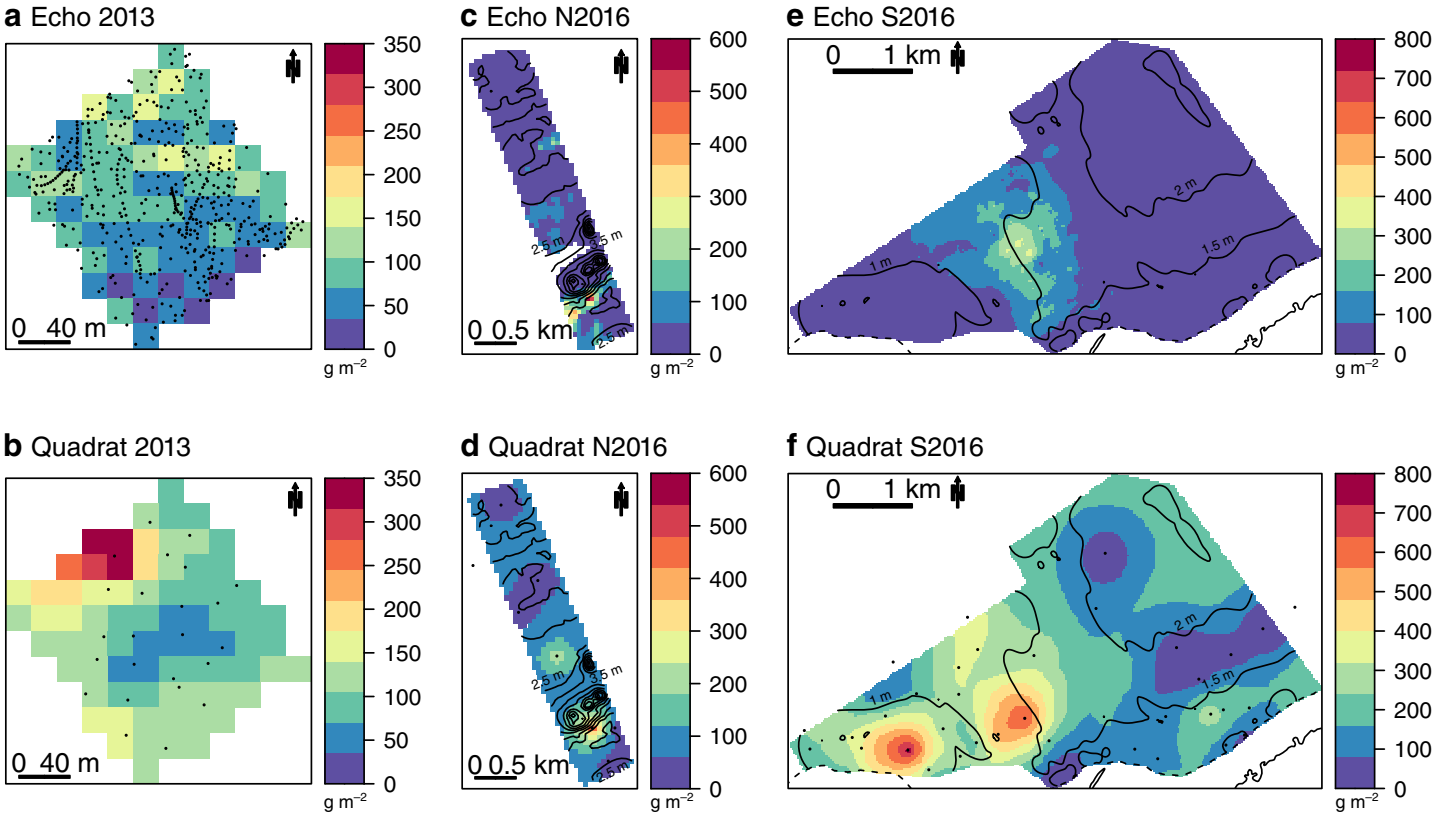

Fig. 6. Comparison of spatially interpolated quadrat-equivalent biomass estimated from echosounding (top panels) and point measurements (bottom panels). (**a**,**b**) 2013 small-scale plot of constant depth, (**c**,**d**) North section of LSP with depths ranging from 0.5 to 7 m sampled in 2016, (**e**,**f**) South section of LSP with shallow depths (< 2.5 m). Lines are isobaths at 0.5 m increments and dots sampled sites (not displayed for clarity in **c**,**e**).

echosounding generated more precise estimates with smaller confidence intervals compared to the very large uncertainty associated with the rake estimation. In contrast to the difference between techniques, spatial interpolation of biomass derived from echosounding did not affect whole-system mean biomass that was very similar to direct estimation from the original echosounding track. Largest differences between estimates were observed for surveys with interrupted echosounding tracks (2013, 2017) that consequently were not covering the study area in a uniform manner (Supporting Information Fig. S5).

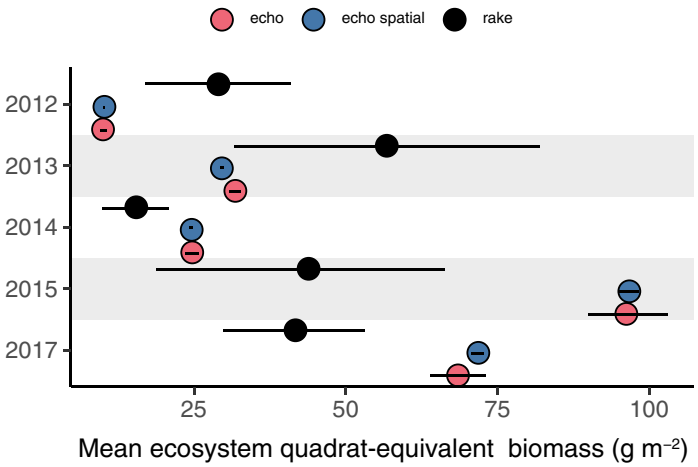

Fig. 7. Comparison of whole-system average quadrat-equivalent biomass using non-spatial predictions from rake and echosounding and spatially interpolated echosounding predicted biomass for five summertime yearly surveys. Horizontal bars represent 95% bootstrapped confidence intervals.

Discussion

We successfully developed two intercalibrations that allow for the interchangeable use of quadrat, rake and echosounding techniques to estimate SAV biomass. We first predicted quadrat biomass from rake biomass and showed the effect of substrate and species growth form on the predictions. Using a resolution of 20 m, we predicted rake biomass from biovolume, a proxy of biomass derived from echosounding. We also showed that this prediction is affected by multiple environmental variables, including SAV growth form, flow velocity, depth, wind conditions and acoustic data quality. By sequentially applying both models to echosounding tracks, we were able to accurately predict quadrat biomass. Since the bias of rake collection can be corrected, this faster and safer

technique could thus be used instead of quadrats as the ground truth for echosounding, particularly when assessing SAV biomass in large areas. In rugged and deeper bottoms, echosounding outperformed point sampling techniques in estimating biomass, but underestimated biomass in very shallow waters. Use of echosounding combined with the intercalibrations are particularly useful at large spatial scales as the higher sampling effort from the greater number of observations provided by this technology increase accuracy by capturing SAV heterogeneity.

Intercalibration between quadrat and rake

Our intercalibration between quadrat and rake biomass confirmed that the two techniques are comparable, and that bias introduced by rake sampling can be corrected (Rodusky et al. 2005; Kenow et al. 2007; Johnson and Newman 2011). This correction is important and meaningful, since failure to correct biomass estimation from the rake can lead to a fourfold underestimation of biomass, with even greater bias at low biomass. In real-world application, the correction can modify sample distribution which can reveal significant differences or patterns in space and time that would not be detected otherwise. Given that the correction is stronger below a rake biomass of 100 g m^{-2}, these effects will depend on the measured rake biomass ranges. The model error was also lower than the standard error of the measured quadrat biomass and was equivalent to the error associated with rake biomass collection. The smaller error and variance of rake were probably caused by the larger rake sample unit size that dampened small-scale heterogeneity captured by quadrat, which had consistently higher ratio of variance to mean biomass. Thus, a gain in accuracy, did not come at the expense of precision.

Our finding that rake collection underestimated biomass confirms previous observations on rake and quadrat comparisons (Rodusky et al. 2005; Kenow et al. 2007; Johnson and Newman 2011). This bias is probably introduced by saturation of plant material on the rake or to the loss of this material as it is lifted from the water. Work by Masto et al. (2020), who combined quadrat–rake apparatus and picked up remaining plant material after rake collection, also suggests that the rake does not completely break plant material at the sediment surface. This harvesting efficiency from rake was affected by the same factors explaining SAV anchorage strength from the natural pulling forces of waves, current or bird foraging: the size of SAV root system and sediment cohesive strength (Schutten et al. 2005). Indeed, we found that canopy-forming SAV tended to be more efficiently collected by rake in contrast to the rosette-forming *V. americana*. The latter has one of the higher root to shoot ratios among freshwater SAV (Stevenson 1988), thus being harder to break from the sediment and being systematically underestimated by the rake. We also observed that the rosette-forming linear leaves tended slip in between rake teeth compared to the canopy-forming that were entangled in them. Additionally, canopy-forming SAV not only tend to have a reduced root system, but their intertwined stem could drag plant material from outside the rake sampled area. Dense stands of the canopy-forming species *Ceratophyllum demersum*, *Potamogeton zosteriformi*, and *Hydrilla verticillata* have previously been overestimated by rake techniques (Rodusky et al. 2005; Johnson and Newman 2011).

Our results further indicate that rake harvesting efficiency is dependent on the substrate type. We found that the rake technique failed to collect any SAV in hard packed sediments (pebble-clay), which provide higher anchorage strength. Counterintuitively, plants were more easily and consistently pulled out from moderately compacted (sand) than from organic and soft sediments (silt). This finding could be an artifact of the more restricted biomass range measured from siltier sites as compared to sandier ones in our survey. However, Rodusky et al. (2005) similarly found a weaker relationship with quadrat biomass and a lower slope when rake collection was on peat-like organic sediments compared to sand. In very loose and organic sediments, the rake could have less grip and SAV be more elusive, being dragged and buried in mud by the rake motion. SAV is also likely more dispersed in this type of substrate since it is not optimal for their growth (Barko et al. 1991). All of these effects would result in less consistent rake harvest in organic substrates. Therefore, calibration of rake biomass measurements could include both species and substrate information to increase accuracy. Nevertheless, we provide a generalized relationship that can be used to derive community level estimate. We also have shown that the calibration is not impacted by the sampling strategy and the depth of the quadrat and rake comparison. Investigators can thus use the simplest sampling strategy, such as the haphazard pair, and reduce sampling effort in deeper more hazardous areas for scuba diving.

Intercalibration between rake and echosounding

We also successfully developed an intercalibration between rake biomass and biovolume. Quadrat biomass has previously been related to biovolume or height measured by echosounder (Maceina et al. 1984; Duarte 1987; Thomas et al. 1990), but to our knowledge, only Howell and Richardson (2019) related rake biomass to biovolume. However, their biovolume was derived from a cloud-based data-processing platform and was not an absolute volumetric estimate; rather it referred to the percent volume inhabited by SAV in the water column (PVI, % cover/depth * height; Thomas et al. 1990; Winfield et al. 2007). This metric is not appropriate to estimate biomass because it is a depth-standardized measurement that does not reflect variation in plant height. For example, given a surface cover of 100%, the same PVI of 80% is measured for a plant height of 2.4 m at a depth of 3 m (2.4/3 * 100) or a height of 0.8 m at a depth of 1 m (0.8/1 * 100). Comparison of these specimens' biomass would likely be very different given their

threefold size difference. Thus, care must be taken when blindly applying measure from the manufacturer; the use of the simple biovolume as % cover multiplied by height is recommended to compare with biomass estimates.

We computed a generalized relationship between rake biomass and biovolume that allowed us to validate the sequential application of rake-echosounding and quadrat–rake models. However, the echosounding and rake relationship was affected by several environmental variables, notably SAV growth form. Indeed, Duarte (1987) has previously shown that given their different biomass allocation with height, deriving calibration by SAV growth form increase accuracy in quadrat biomass estimation. Although not detected in our model, filamentous algae could further introduce bias in the biovolume-rake biomass relationship since they can be detected by echosounder (Depew et al. 2009; Bučas et al. 2016). Predictions were also affected by environmental conditions during sampling, with clear effects of flow velocity, depth and wind direction. The depth and flow effects could be due to differences in species composition that tend to vary by depth or decrease in biomass in deeper areas more exposed to faster flow at our study site (Hudon 1997). Alternatively, underestimation in shallow areas could be due to detection problems either because of an overestimation of bottom depth, which is used to calculate plant height, or of floating plant material at the water surface that was not detected by the echosounder. Observations when wind was coming from North to North-West also overestimated biovolume. In LSP, winds coming from this direction go against water current and are in the general orientation of the lake, which increases the traveling distance on open water. Both of these factors can increase wave height and create bubbles that cause false echosounding plant detection. To account for these environmental variations, greater accuracy could be provided by conducting a calibration per sampling campaign (Figure 4a), for similar environmental conditions or during favorable wind conditions.

Versatility of using two intercalibrations

Compared to the application of a single technique, our two intercalibration approach allows for more versatility and the measurement of SAV biomass at wider temporal and spatial scales. We provide in Fig. 8 a step-by-step guideline composed of key questions that help decide when only quadrat collection, the rake–quadrat intercalibration or the full two-step intercalibration is best suited. First, the choice of the method should be guided by the desired spatial and temporal scale of inquiry. When sampling effort is low, quadrats are likely to be the first technique of choice given its accuracy. Although accurate, collecting biomass from quadrats is rarely conceivable. Indeed, given that scuba-diving can be a life-threatening activity, it is increasingly regulated by institutions who establish strict safety protocols and limit its use. Rake becomes an interesting alternative as it can limit scuba-diving to a one-time event for the determination of the quadrat–rake intercalibration. In addition, the use of rake saves time since that, depending on the diver's experience, a single quadrat collection can take up to half an hour (Downing and Anderson 1985) compared to a few minutes for rake. Time and resources gained by using the rake in combination with the improved underwater accessibility can be dedicated to additional sample collection, thus improving sample size, the understanding of SAV diversity, and spatial coverage.

If a larger spatial and temporal resolution is required, echosounding likely becomes the technique of choice. The major impediment to apply echosounding would be its high purchase cost and the necessity to postprocess results. These can be reduced by considering the use of a consumer-grade echosounder coupled to cloud-based automated data-processing tools (Munday et al. 2013; Helminen et al. 2019; Howell and Richardson 2019). Once echosounding is chosen, it also requires a ground truthing as it only provides a proxy of biomass. Quadrats could be used for this purpose (Duarte 1987), and given the safety issues and cumbersomeness of the techniques it should be considered only if very few samples are needed. Rake and our two-step intercalibration approach would likely be more appropriate as rake is simpler, safer and faster to sample. Using rake as a ground truth enables echosounding to cover large extents of SAV meadows in a uniform manner, thus capturing more of the spatial heterogeneity and increasing biomass accuracy at the ecosystem scale. In our whole-system estimation, the different sampling efforts yielded incomparable biomass between techniques. Although the precision of biomass predictions from echosounding at an individual site is lower than that of rake, that loss is counteracted by the sheer number of echosounding measurements. Achieving a similar sampling effort with the rake technique would be impossible. We estimated that it would take 60 days using a rake to simply collect a similar ecosystem-scale sample areal extent of the echosounder as observed in Fig. 7, without taking into account processing time. We also saw that there is no real gain in using spatial interpolation techniques to estimate biomass if there is a thorough coverage of the study area with echosounding. This is more effective as it requires less post-processing and computing power. Furthermore, using the rake in combination with echosounding provides information on SAV species that is not available using echosounding. Using the two techniques also allows to increase the available depth range as rake samples are suitable in very shallow areas and echosounding in deeper ones.

Our approach also allows for retrospective decisions with a change in priorities. For example, many existing monitoring programs rely on rake measurements (e.g., Rodusky et al. 2005; Yin and Kreiling 2011). If more rapid sampling or higher coverage is needed, our approach could facilitate the substitution of rake technique with echosounding. To do so we provide an intercalibration that allows for this comparison, but we also point out that the ecosystem-scale biomass estimation

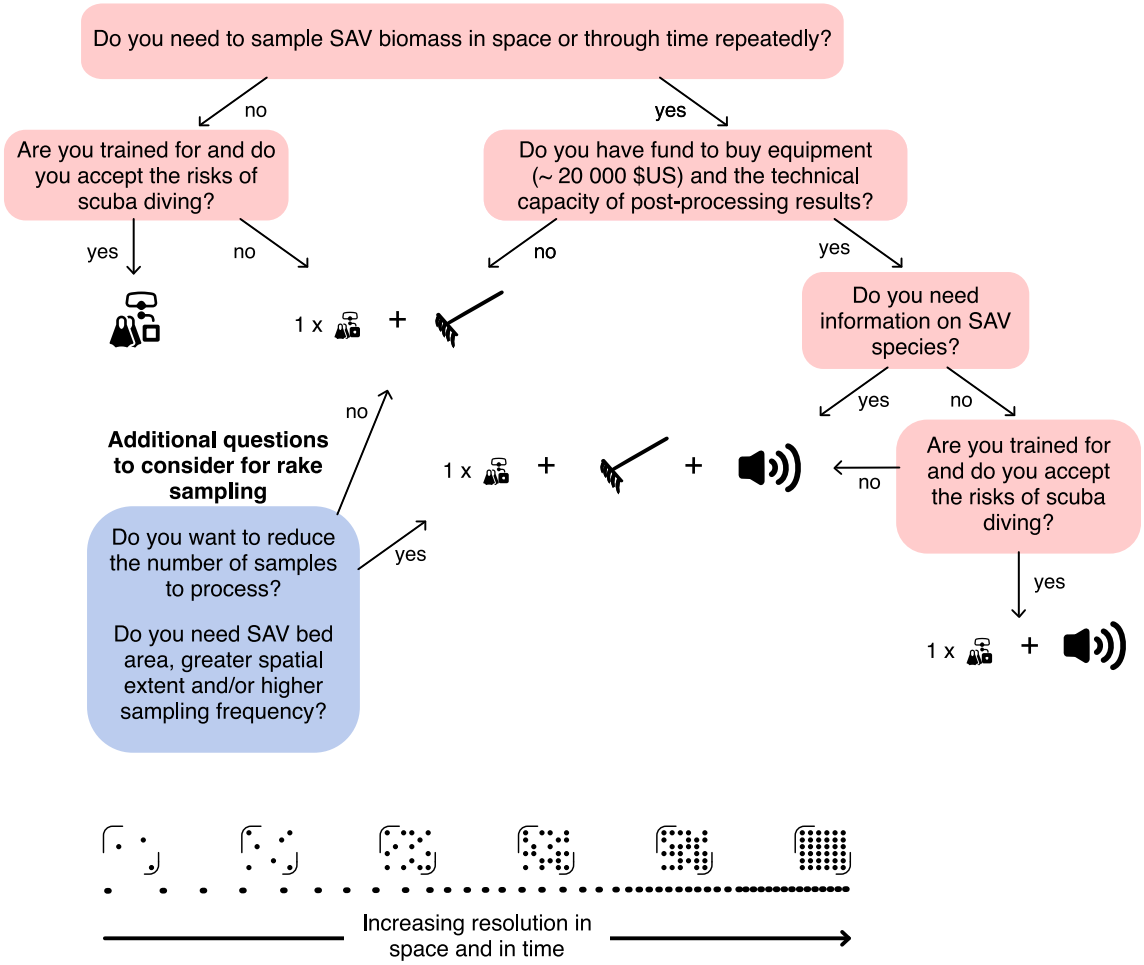

Fig. 8. Step-by-step guideline to decide what biomass method to use and when combining them is desirable.

depends on the sampling effort, which is inherently higher with echosounding. Thus, to have reliable SAV biomass trends through time, only the sites that were continuously sampled should be compared. This mean that a subset of the echosounding data, that would likely cover a greater area than rake sites, should be used for this temporal analysis.

Comments and recommendations

The choice to use one or both intercalibrations will depend on the study goals, resources available and time granted. If one only intends to use rake, the quadrat and rake calibration can be conducted using the simplest sampling strategy, where only a one-time calibration is needed, with sites chosen to maximize a biomass gradient and ensure divers security. Increased accuracy can be achieved by deriving species- and substrate-specific equations. For the rake and echosounding combination, an even more efficient intercalibration can be achieved than the one presented here. For example, despite having a rake dataset of 217 sites, we only had 52 sites that spatially matched the echosounding tracks at 10 m radius resolution. Since the two sampling techniques were not used simultaneously, sampling with both techniques had to be conducted as close as possible to an assigned geographic position. Over the 6-yr sampling period, variations in staff and GPS accuracy resulted in reduced precision, yielding a lower number of matched pairs in later years, which affected predictions (Fig. 4c). These shortcomings can be overcome by conducting the rake sampling and echosounding simultaneously. For example, buoys could be deployed as the echosounder is passing over the selected calibration sites for subsequent rake collection. Furthermore, when dense plant material is floating at the water surface, echosounding is inappropriate: the transducer is blinded which leads to drastically underestimated biomass. In contrast, the rake is not appropriate in deep waters (> 3–4 m) where other apparatus and collection strategies should be tested and compared to either quadrats or echosounding. Therefore, to maximize matched rake-echosounding sites and avoid sampling in inappropriate conditions, careful planning of sampling and training of field technicians are necessary.

Information needed regarding species composition, substrate type and time dedicated for biomass samples or echosounding postprocessing should also be planned in advance. The rake has the advantage of providing species information, but each sample entails considerable sample processing time. Using a faster semi-quantitative approach such as applying a visual abundance scale based on the degree of each species filling the rake teeth can help increase sample size and provide community information at the ecosystem scale (Yin and Kreiling 2011), which can be used to more accurately predict biomass. When different SAV communities display distinctive heights, for example understory charophytes and taller angiosperms, applying height threshold to echosounding data can provide functional group information at large spatial scales (Bučas et al. 2016). Recent echosounders also provide information on substrate type that can increase accuracy when applying our two-step calibration approach (Munday et al. 2013; Helminen et al. 2019). New technological development in hydroacoustic autonomous boats (Goulon et al. 2021) are further promising to reduce sampling time and increase sampling frequency. To confirm that the inter-calibration we provide can be generalized, comparison of biomass techniques should additionally be conducted in other environments and using a diversity of apparatus such as different tools to sample SAV from the surface or echosounder frequencies. Given the technological progress that were accomplished over the past decade, it is likely that future developments in GPS, echosounding and computing power will further facilitate and decrease costs related to large-scale estimations of SAV biomass over a wide range of environmental conditions.

Data availability statement

The data that support the findings of this study are openly available in Zenodo at link https://doi.org/10.5281/zenodo.7622140.

References

Barko, J. W., D. Gunnison, and S. R. Carpenter. 1991. Sediment interactions with submersed macrophyte growth and community dynamics. Aquat. Bot. **41**: 41–65. doi:10.1016/0304-3770(91)90038-7

Bartoń, K. 2020. MuMIn: Multi-model inference. R package version 1.43.17. Available from https://CRAN.R-project.org/package=MuMIn

Bates, D., M. Maechler, B. Bolker, and S. Walker. 2015. Fitting linear mixed-effects models using lme4. J. Stat. Softw. **67**: 1–48.

Brown, J. H., J. F. Gillooly, A. P. Allen, V. M. Savage, and G. B. West. 2004. Toward a metabolic theory of ecology. Ecology **85**: 1771–1789. doi:10.1890/03-9000

Bučas, M., A. Šaškov, A. Šiaulys, and Z. Sinkevičienė. 2016. Assessment of a simple hydroacoustic system for the mapping of macrophytes in extremely shallow and turbid lagoon. Aquat. Bot. **134**: 39–46. doi:10.1016/j.aquabot.2016.06.009

Canty, A., and B. Ripley. 2021. boot: Bootstrap R (S-plus) functions. R package version 1.3-28.

Carpenter, S. R., and D. M. Lodge. 1986. Effects of submersed macrophytes on ecosystem processes. Aquat. Bot. **26**: 341–370. doi:10.1016/0304-3770(86)90031-8

Cattaneo, A., C. Hudon, C. Vis, and P. Gagnon. 2013. Hydrological control of filamentous green algae in a large fluvial lake (Lake Saint-Pierre, St. Lawrence River, Canada). J. Great Lakes Res. **39**: 409–419. doi:10.1016/j.jglr.2013.06.005

Cyr, H., and J. A. Downing. 1988. The abundance of phytophilous invertebrates on different species of submerged macrophytes. Freshw. Biol. **20**: 365–374. doi:10.1111/j.1365-2427.1988.tb00462.x

Depew, D. C., A. W. Stevens, R. E. H. Smith, and R. E. Hecky. 2009. Detection and characterization of benthic filamentous algal stands (*Cladophora* sp.) on rocky substrata using a high-frequency echosounder. Limnol. Oceanogr. Methods **7**: 693–705. doi:10.4319/lom.2009.7.693

Downing, J. A., and M. R. Anderson. 1985. Estimating the standing biomass of aquatic macrophytes. Can. J. Fish. Aquat. Sci. **42**: 1860–1869. doi:10.1139/f85-234

Duarte, C. M. 1987. Use of echosounder tracings to estimate aboveground biomass of submerged plants in lakes. Can. J. Fish. Aquat. Sci. **44**: 732–735. doi:10.1139/f87-088

Duarte, C. M., and J. Kalff. 1990. Patterns in the submerged macrophyte biomass of lakes and the importance of the scale of analysis in the interpretation. Can. J. Fish. Aquat. Sci. **47**: 357–363. doi:10.1139/f90-037

Farrés, M., S. Platikanov, S. Tsakovski, and R. Tauler. 2015. Comparison of the variable importance in projection (VIP) and of the selectivity ratio (SR) methods for variable selection and interpretation. J. Chemometr. **29**: 528–536. doi:10.1002/cem.2736

Gombin, J., Vaidyanathan, R. and V. Agafonkin 2020. concaveman: A very fast 2D concave Hull algorithm. R package version 1.1.0. Available from https://CRAN.R-project.org/package=concaveman

Goulon, C., O. Le Meaux, R. Vincent-Falquet, and J. Guillard. 2021. Hydroacoustic Autonomous boat for Remote fish detection in LakE (HARLE), an unmanned autonomous surface vehicle to monitor fish populations in lakes. Limnol. Oceanogr. Methods **19**: 280–292. doi:10.1002/lom3.10422

Helminen, J., T. Linnansaari, M. Bruce, R. Dolson-Edge, and R. A. Curry. 2019. Accuracy and precision of low-cost echosounder and automated data processing software for habitat mapping in a large river. Diversity **11**: 116. doi:10.3390/d11070116

Hijmans, R. J. 2020. raster: Geographic data analysis and Modeling. R package version 3.4-5. Available from https://CRAN.R-project.org/package=raster

Hilt, S., S. Brothers, E. Jeppesen, A. J. Veraart, and S. Kosten. 2017. Translating regime shifts in shallow lakes into changes in ecosystem functions and services. Bioscience **67**: 928–936. doi:10.1093/biosci/bix106

Howell, A. W., and R. J. Richardson. 2019. Correlation of consumer grade hydroacoustic signature to submersed plant biomass. Aquat, Bot. **155**: 45–51. doi:10.1016/j.aquabot.2019.02.001

Hudon, C. 1997. Impact of water level fluctuations on St. Lawrence River aquatic vegetation. Can. J. Fish. Aquat. Sci. **54**: 2853–2865. doi:10.1139/f97-201

Hudon, C., and others. 2012. Oligotrophication from wetland epuration alters the riverine trophic network and carrying capacity for fish. Aquat. Sci. **74**: 495–511. doi:10.1007/s00027-011-0243-2

Hussner, A., and others. 2017. Management and control methods of invasive alien freshwater aquatic plants: A review. Aquat. Bot. **136**: 112–137. doi:10.1016/j.aquabot.2016.08.002

Johnson, J. A., and R. M. Newman. 2011. A comparison of two methods for sampling biomass of aquatic plants. J. Aquat. Plant Manage. **49**: 1–8.

Johnson, M. P. 2020. Estimating intertidal seaweed biomass at larger scales from quadrat surveys. Mar. Environ. Res. **156**: 104906. doi:10.1016/j.marenvres.2020.104906

Kenow, K. P., J. E. Lyon, R. K. Hines, and A. Elfessi. 2007. Estimating biomass of submersed vegetation using a simple rake sampling technique. Hydrobiologia **575**: 447–454. doi:10.1007/s10750-006-0284-z

Maceina, M. J., J. V. Shireman, K. A. Langeland, and D. E. Canfield. 1984. Prediction of submersed plant biomass by use of a recording fathometer. J. Aquat. Plant Manage. **22**: 35–38.

Madsen, J. D. 1993. Biomass techniques for monitoring and assessing control of aquatic vegetation. Lake Reserv. Manage. **7**: 141–154. doi:10.1080/07438149309354266

Madsen, J. D., and R. M. Wersal. 2017. A review of aquatic plant monitoring and assessment methods. J. Aquat. Plant Manage. **55**: 1–12.

Masto, N. M., B. A. Bauer, R. M. Kaminski, C. Sharpe, R. C. Leland, E. Wiggers, and P. D. Gerard. 2020. Rake Sampling to Estimate Biomass of Submersed Aquatic Vegetation in Coastal Wetlands. Wetlands **40**: 957–966. doi:10.1007/s13157-020-01296-3

Mehmood, T., K. H. Liland, L. Snipen, and S. Sæbø. 2012. A review of variable selection methods in partial least squares regression. Chemom. Intel. Lab. Syst. **118**: 62–69. doi:10.1016/j.chemolab.2012.07.010

Mevik, B.-H., and R. Wehrens. 2007. The pls package: Principal component and partial least squares regression in R. J. Stat. Softw. **18**: 23. doi:10.18637/jss.v018.i02

Mevik, B.-H., R. Wehrens, and K. H. Liland 2020. pls: Partial least squares and principal component regression. R package version 2.7-3. Available from https://CRAN.R-project.org/package=pls

Munday, E., B. Moore, and J. Burczynski. 2013. Hydroacoustic mapping system for quantitative identification of aquatic macrophytes, substrate composition, and shallow water bathymetric surveying, p. 1–3. *In* 2013 OCEANS, San Diego. doi:10.23919/OCEANS.2013.6741196

Pebesma, E. 2018. Simple features for R: Standardized support for spatial vector data. R J. **10**: 439–446. doi:10.32614/RJ-2018-009

Pebesma, E. J. 2004. Multivariable geostatistics in S: The gstat package. Comput. Geosci. **30**: 683–691. doi:10.1016/j.cageo.2004.03.012

Pebesma, E.J. and R.S. Bivand, 2005. Classes and methods for spatial data in R. R News **5**. Available from https://cran.r-project.org/doc/Rnews/

R Core Team (2020). R: A language and environment for statistical computing. R Foundation for Statistical Computing. Available from https://www.r-project.org/

Rodusky, A. J., B. Sharfstein, T. L. East, and R. P. Maki. 2005. A comparison of three methods to collect submerged aquatic vegetation in a shallow lake. Environ. Monit. Assess. **110**: 87–97. doi:10.1007/s10661-005-6338-2

Rooney, N., J. Kalff, and C. Habel. 2003. The role of submerged macrophyte beds in phosphorus and sediment accumulation in Lake Memphremagog, Quebec, Canada. Limnol. Oceanogr. **48**: 1927–1937. doi:10.4319/lo.2003.48.5.1927

Rowan, G. S. L., and M. Kalacska. 2021. A review of remote sensing of submerged aquatic vegetation for non-specialists. Remote Sens. (Basel) **13**: 623. https://www.mdpi.com/2072-4292/13/4/623

Sabol, B. M., R. E. Melton, R. Chamberlain, P. Doering, and K. Haunert. 2002. Evaluation of a digital echo sounder system for detection of submersed aquatic vegetation. Estuaries **25**: 133–141. doi:10.1007/bf02696057

Scheffer, M., S. H. Hosper, M. L. Meijer, B. Moss, and E. Jeppesen. 1993. Alternatives equilibria in shallow lakes. Trends Ecol. Evol. **8**: 275–279. doi:10.1016/0169-5347(93)90254-m

Schutten, J., J. Dainty, and A. J. Davy. 2005. Root anchorage and its significance for submerged plants in shallow lakes. J. Ecol. **93**: 556–571. doi:10.1111/j.1365-2745.2005.00980.x

Stevenson, J. C. 1988. Comparative ecology of submersed grass beds in freshwater, estuarine, and marine environments. Limnol. Oceanogr. **33**: 867–893. doi:10.4319/lo.1988.33.4part2.0867

Thomas, G. L., S. L. Thiesfeld, S. A. Bonar, R. N. Crittenden, and G. B. Pauley. 1990. Estimation of submergent plant bed biovolume using acoustic range information. Can. J. Fish. Aquat. Sci. **47**: 805–812. doi:10.1139/f90-093

Vis, C., C. Hudon, and R. Carignan. 2003. An evaluation of approaches used to determine the distribution and biomass of emergent and submerged aquatic macrophytes over large spatial scales. Aquat. Bot. **77**: 187–201. doi:10.1016/s0304-3770(03)00105-0

Winfield, I. J., and others. 2007. Assessment in two shallow lakes of a hydroacoustic system for surveying aquatic macrophytes. Hydrobiologia **584**: 111–119. doi:10.1007/s10750-007-0612-y

Yin, Y., and R. M. Kreiling. 2011. The evaluation of a rake method to quantify submersed vegetation in the Upper Mississippi River. Hydrobiologia **675**: 187–195. doi:10.1007/s10750-011-0817-y

Zuur, A. F., E. N. Ieno, N. J. Walker, A. A. Saveliev, and G. M. Smith. 2009. Mixed effects models and extensions in ecology and extentions in ecology with R. Springer Science +Business Media.

Acknowledgments

The authors thank Stéphanie Massé, Caroline Chartier, Elena Neszvecsko, Geneviève Trottier, Magalie Noiseux-Laurin and François Messier from GRIL, Patricia Bolduc from UQTR and all other students that conducted field work and processed samples. The technical support of Jean-Pierre Amyot, Conrad Beauvais, Rollando Benjamin, Maude Lachapelle, Yasmina Remmal and Maxime Wauthy from Environment Canada is acknowledged with thanks. Bruce Gray and the Technical Operations diving team (Environment and Climate Change Canada, Canada Centre for Inland Waters, Burlington, ON) provided excellent field support for underwater sample collection. The authors also thank Richard Carignan and Andrea Bertolo for planning and troubleshooting during echosounding surveys. We thank Lars Iversen, Sabine Hilt, and two anonymous reviewers for insightful comments that improved the manuscript. Sampling was made possible thanks to the guides from pourvoirie Roger Gladu. This project was funded by the GRIL, a FRQNT Initiatives stratégiques pour l'innovation grant, FRQNT and NSERC scholarships to MB. This work was supported by Environment and Climate Change Canada (ECCC) as part of the Canada-Québec St. Lawrence Action Plan (SLAP) (CH).

Submitted 22 November 2022
Accepted 07 February 2023

Associate editor: Scott Ensign